In the decay of both Tm^{166} and Tm^{168} to the even-even isotopes of Er^{166} and Er^{168}, highly populated members of a $K=2+$ vibrational band are observed.[3] These levels are characteristically found at 750 to 1000 kev and decay to the levels of the ground-state rotational band by the emission of gamma rays of 600 to 900 kev. No gamma rays in this energy range were observed with the scintillation spectrometer following the decay of either Tm^{164} or Tm^{162}.

[3] K. P. Jacob, J. W. Mihelich, B. Harmatz, and T. H. Handley, Phys. Rev. **117**, 1102 (1960); R. G. Wilson and M. L. Pool, Phys. Rev. **119**, 262 (1960).

PHYSICAL REVIEW VOLUME 120, NUMBER 5 DECEMBER 1, 1960

Measurements of Spatial Asymmetries in the Decay of Polarized Neutrons*

M. T. Burgy, V. E. Krohn,† T. B. Novey, and G. R. Ringo
Argonne National Laboratory, Argonne, Illinois

and

V. L. Telegdi
University of Chicago, Chicago, Illinois

(Received July 22, 1960)

A series of experiments has been carried out to examine the spatial symmetry properties of the beta decay of the free neutron. Measurements of angular distributions of the electrons and protons coming from the decay of polarized neutrons have shown that the correlation coefficient between the directions of electron momentum and neutron spin is -0.11 ± 0.02 and that between the antineutrino momentum and the neutron spin is 0.88 ± 0.15. The coefficient of the term proportional to the scalar triple product of antineutrino momentum, electron momentum, and neutron spin (which is not invariant under time reversal) is 0.04 ± 0.05. All these results are consistent with the $A-V$ theory of beta decay. Details of measurement techniques and the method of producing a beam of polarized neutrons are given.

I. INTRODUCTION

BESIDES the decay rate λ and the spectrum $N(p_e)$, the fundamental process of beta decay,

$$n \rightarrow p+e+\bar{\nu}, \tag{1}$$

is further characterized by certain angular correlations (asymmetries) between such physically observable quantities as the spins and momenta of the particles involved. A complete theory of beta decay should predict all of these observable effects quantitatively. Conversely, the empirical knowledge of all such correlations (in addition to that of the decay rate and of the spectrum) should specify, and possibly overdetermine, all the free parameters of the theory (i.e., the so-called coupling constants). The fact that the neutron undergoing beta decay is, in most experiments, embedded in nuclear matter should not affect this statement. However in order to interpret such experiments, one must have a valid description of nuclear structure. Lacking this knowledge, further free parameters (i.e., the nuclear matrix elements) appear in the theoretical predictions for the observable effects, without essentially increasing the number of experimentally observable quantities.

At the time of the discovery of the breakdown of invariance under space inversion (P) and charge conjugation (C) in weak interactions,[1] Robson and others[2] had already shown that measurements on the decay of free neutrons are experimentally feasible. We therefore decided to investigate in this process those asymmetries which arise from the failure of P and C invariance, and also a particular asymmetry which could arise[3] if time-reversal invariance (T) also failed in beta decay.

The probability of emission of electrons and antineutrinos from polarized nuclei is given by Jackson, Treiman, and Wyld[3] as

$$\omega(\langle\mathbf{J}\rangle E_e,\Omega_e,\Omega_{\bar{\nu}})dE_e d\Omega_e d\Omega_{\bar{\nu}}=\frac{1}{(2\pi)^5}p_e E_e(E^0-E_e)^2$$
$$\times dE_e d\Omega_e d\Omega_{\bar{\nu}}\xi\Big\{1+a\frac{\mathbf{p}_e\cdot\mathbf{p}_{\bar{\nu}}}{E_e E_{\bar{\nu}}}+b\frac{m}{E_e}$$
$$+c\Big[\frac{1}{3}\frac{\mathbf{p}_e\cdot\mathbf{p}_{\bar{\nu}}}{E_e E_{\bar{\nu}}}-\frac{(\mathbf{p}_e\cdot\mathbf{j})(\mathbf{p}_{\bar{\nu}}\cdot\mathbf{j})}{E_e E_{\bar{\nu}}}\Big]\Big[\frac{J(J+1)-3\langle(\mathbf{J}\cdot\mathbf{j})^2\rangle}{J(2J+1)}\Big]$$
$$+\frac{\langle\mathbf{J}\rangle}{J}\cdot\Big[\mathfrak{A}\frac{\mathbf{p}_e}{E_e}+\mathfrak{B}\frac{\mathbf{p}_{\bar{\nu}}}{E_{\bar{\nu}}}+\mathfrak{D}\frac{\mathbf{p}_e\times\mathbf{p}_{\bar{\nu}}}{E_e E_{\bar{\nu}}}\Big]\Big\}. \tag{2}$$

* Work performed under the auspices of the U. S. Atomic Energy Commission.

† Presently at Ramo-Wooldridge, Canoga Park, California.

[1] C. S. Wu, E. Ambler, R. W. Hayward, D. D. Hoppes, and R. P. Hudson, Phys. Rev. **105**, 1413 (1957); R. L. Garwin, L. M. Lederman, and M. Weinrich, Phys. Rev. **105**, 1416 (1957); J. I. Friedman and V. L. Telegdi, Phys. Rev. **105**, 1681 (1957).

[2] J. M. Robson, Phys. Rev. **83**, 349 (1951); A. H. Snell, F. Pleasonton, and R. V. McCord, Phys. Rev. **78**, 310 (1950).

[3] J. D. Jackson, S. B. Treiman, and H. W. Wyld, Phys. Rev. **106**, 517 (1957).

For the case of the neutron, $J(J+1)-3\langle(\mathbf{J}\cdot\mathbf{j})^2\rangle=0$. If we assume the absence of Fierz interference terms ($b=0$) then this becomes

$$\omega=N(E)\xi\left\{1+a\frac{\mathbf{p}_e\cdot\mathbf{p}_{\bar\nu}}{E_eE_{\bar\nu}}+\mathfrak{A}\frac{\langle\mathbf{J}\rangle}{J}\cdot\frac{\mathbf{p}_e}{E_e}+\mathfrak{B}\frac{\langle\mathbf{J}\rangle}{J}\cdot\frac{\mathbf{p}_{\bar\nu}}{E_{\bar\nu}}+\mathfrak{D}\frac{\langle\mathbf{J}\rangle}{J}\cdot\frac{\mathbf{p}_e}{E_e}\times\frac{\mathbf{p}_{\bar\nu}}{E_{\bar\nu}}\right\}. \quad (3)$$

Thus ω depends upon the solid angles for the detection of the particles involved, their energies, and the direction and magnitude of neutron polarization. By judicious selection of the experimental arrangement, the contribution of each term may be isolated. The term proportional to $\mathbf{p}_e\cdot\mathbf{p}_{\bar\nu}$ has been studied previously[4] and, although very difficult to measure, was known to be small.

The last three terms suggest three experiments requiring polarized neutrons:

(1) The electron up-down asymmetry, of the form

$$1+\mathfrak{A}(\langle\mathbf{J}\rangle/J)\cdot(\mathbf{p}_e/E_e).$$

(2) The antineutrino up-down asymmetry, of the form

$$1+\mathfrak{B}(\langle\mathbf{J}\rangle/J)\cdot(\mathbf{p}_{\bar\nu}/E_{\bar\nu}).$$

(3) The neutron-electron-antineutrino correlation, of the form

$$1+\mathfrak{D}(\langle\mathbf{J}\rangle/J)\cdot(\mathbf{p}_e\times\mathbf{p}_{\bar\nu}/E_eE_{\bar\nu}).$$

The scalar product of observables entering the first two correlations is obviously odd under space inversion, while the triple product in the last one is odd under time reversal. The coefficients $\mathfrak{A}$, $\mathfrak{B}$, and $\mathfrak{D}$ depend bilinearly on the free parameters of the theory; their dependence has been given by Jackson, Treiman, and Wyld,[4] and by other authors.[5]

All three correlations involve the neutron spin, i.e., are observed only in the decay of *polarized* neutrons. A method developed several years ago in this laboratory[6] enabled us to obtain an intense beam of almost completely polarized thermal neutrons under very favorable background conditions. The methods used in producing and analyzing this beam, as well as other experimental matters common to all three asymmetry measurements, will be described in Sec. II. Sections III, IV, and V cover experimental matters specific to each of the three correlation experiments. In Sec. VI, we discuss the consequences of our results for the theory of beta decay. While this work was in progress or available only in preliminary form,[7] many experiments[8] on complex nuclei were carried out. These corroborate or amplify the conclusions that may be drawn from our results.

II. APPARATUS

A. Cobalt-Iron Mirror

The experimental arrangements in these measurements were generally as shown in Fig. 1. The neutrons used were obtained from the Argonne Research Reactor, CP-5, in a beam from a collimator $85\frac{3}{4}$ in. long, 8 in. high, and $\frac{1}{4}$ in. wide. After leaving the collimator the beam was polarized by reflection[6] from a mirror of 95% Co and 5% Fe alloy[9] magnetized in a vertical direction by a field of roughly 250 oe. To make this mirror, the Co-Fe alloy was cast and then rolled into a sheet about 0.025 in. thick. Pieces of this sheet were silver soldered onto ten copper blocks 5 in. square and 1 in. thick in a controlled-atmosphere furnace, after which the Co-Fe surfaces were ground and then polished to a flatness of about 3 fringes. The copper blocks were then mounted on a long aluminum bar with their surfaces in the same plane to an accuracy of about 0.001 in. to make a mirror 5 in. high and 50 in. long. The reflectivity of this mirror appears to be about $\frac{3}{4}$ for neutrons of less than the critical velocity and it does not add appreciably to the divergence of the beam.

The beam from the reactor struck the mirror at a grazing angle of about 8 min and then entered a vacuum chamber through the shields shown in the figure. Brass blocks, 1 ft long, were placed about $\frac{1}{8}$ in. from the mirror face at the center and outer end. The effective collimation of the beam was determined by the inner end of the collimator in the reactor ($\frac{1}{4}$ in. wide) and by the mirror. The brass and lead shields, however, served to reduce stray radiation. As a special precaution against gamma rays from neutron capture, the parts of the shield near the beam in the vacuum chamber were made of a lead alloy containing 0.5% Li by weight. The shielding proved to be quite effective as judged by the fact that the gamma-ray level in the beam in the chamber was lower than 100 mr/hr.

The reflected beam contained a total of about 5×10^7 neutrons/sec spread over an area about 8 in. high and $\frac{1}{4}$ in. wide at the point where the neutron decays were observed.

The polarization of the neutron beam was measured by reflection from a second Co-Fe mirror magnetized

[4] J. M. Robson, Can. J. Phys. **36**, 1450 (1958); Yu. V. Trebukhovskii, V. V. Vladimirskii, V. K. Grigoriev, and V. A. Ergakov, J. Exptl. Theoret. Phys. (U.S.S.R.) **36**, 1314 (1959) [translation: Soviet Phys.—JETP **36(9)**, 931 (1959)].

[5] M. E. Ebel and G. Feldman, Nuclear Phys. **4**, 213 (1957); K. Alder, B. Stech, and A. Winther, Phys. Rev. **107**, 728 (1957).

[6] M. Hamermesh, Phys. Rev. **75**, 1766 (1949); D. J. Hughes and M. T. Burgy, Phys. Rev. **81**, 498 (1951).

[7] M. T. Burgy, V. E. Krohn, T. B. Novey, G. R. Ringo, and V. L. Telegdi, Phys. Rev. Letters **1**, 502 (1958); M. T. Burgy, V. E. Krohn, T. B. Novey, G. R. Ringo, and V. L. Telegdi, Phys. Rev. **110**, 1214 (1958).

[8] E. J. Konopinski, in *Annual Reviews of Nuclear Physics*, edited by E. Segrè and I. C. Schiff (Annual Reviews Inc., Palo Alto, California, 1959), Vol. 9, p. 99.

[9] The 5% Fe gives an alloy which has a cubic structure and is magnetically much softer than Co. The added iron does not seriously affect the index of refraction for neutrons of either spin state.

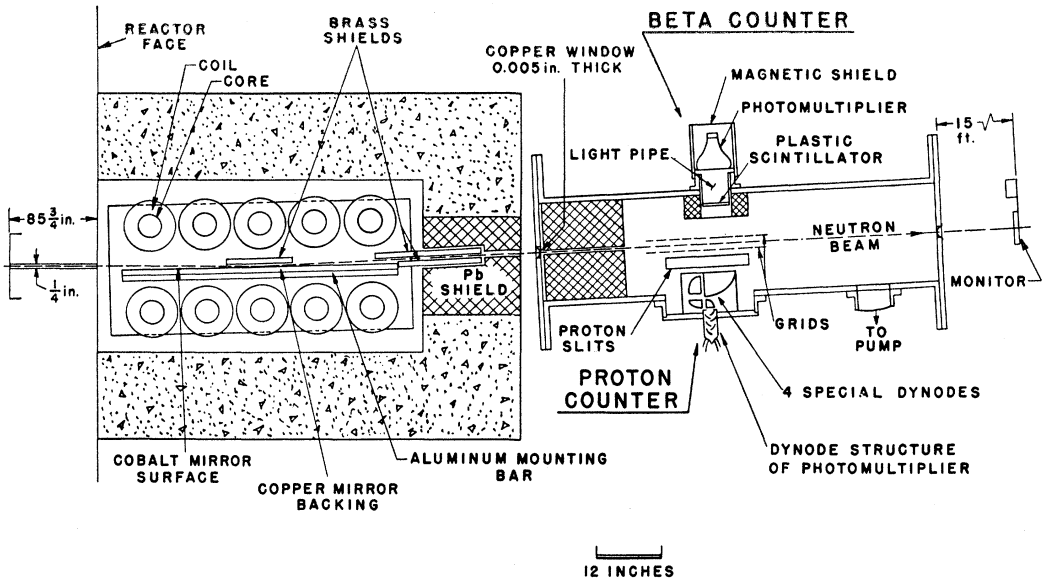

FIG. 1. Horizontal section through center of the apparatus for the study of the decay of polarized neutrons.

in the same direction as the first. This analyzer was placed between the vacuum chamber and the monitor. The measurements of the polarization were made by recording the intensity of the doubly reflected beam with and without an unmagnetized steel sheet about 0.01 in. thick placed in the beam between the polarizer and analyzer. The sheet, which completely depolarized the beam owing to random precessions in its disoriented domains, would reduce the intensity of the second reflection by 50% if polarizer and analyzer were perfect. It actually reduced the intensity by about 43%, which would indicate about 75% polarization. Since the polarizing and analyzing mirrors were essentially identical and in a similar magnetic environment, it is believed that they share the blame for the imperfection of polarization. Hence the beam in between them is believed to have a polarization of 87% with an uncertainty of $\pm 7\%$ which is intended to cover the reasonable range of failure of the assumption of equal imperfection in polarizer and analyzer. The other sources of error in the polarization measurement are relatively small. When measurements of polarization were not in progress, the analyzer was removed since it would have added to the background in the measurements of neutron decay.

In the measurements of polarization and during the decay measurements, it was necessary to have a magnetic guide field of about 2–5 gauss to preserve the magnitude and direction of polarization. This guide field was supplied by a magnetic condenser consisting of two plates, about $\frac{1}{2}$ in. thick and 2 ft wide, running the full length of the vacuum chamber just outside its walls. These were excited by four small coils on two yokes. In practice it was not always necessary to energize the coils continuously since residual fields were sometimes sufficient. The plates used as the poles in the magnetic condenser had holes for the various detectors, pumping lines, ion gauge, etc. These did not significantly perturb the field in the chamber.

B. Vacuum Chamber

The vacuum chamber in which the neutron decays were observed was fabricated of 1-in. aluminum plates welded together, except for the end plates which were made of 1-in. copper to simplify the construction of the thin copper windows. The end plates, the detectors, and several other openings in the chamber were sealed with *O* rings lubricated with Apeizon *T*. The system was pumped by a 6-in. oil diffusion pump. In the line between the chamber and the pump there was a trap cooled with liquid nitrogen. A pressure of about 10^{-6} mm of Hg was usually maintained in the chamber and, in spite of the possible sources of organic contaminants present, the electron multiplier of the proton detector did not show appreciable deterioration in a few months except on the rare occasions when the trap or pump failed.

C. Proton Detector

The neutron decays were detected by coincidences between a proton detector and an electron detector, with an appropriate time delay requirement corresponding to the flight time of the proton. This is the method which had proved quite successful in reducing background in earlier studies of the neutron lifetime.[2]

The protons to be detected were accelerated (to energies of 5 to 10 kev) toward an electron-multiplier system which amplified the secondary electron current emitted when a proton struck a silver-magnesium

surface which served as the cathode of the system. This cathode and the first three dynodes of the multiplier were tapered so that the area of the opening to each stage (and the exit of the previous stage) was about one third as large as the opening of the previous stage. The entrance to the cathode was 6 in. square and the exit from the third dynode was $\frac{5}{8}$ in. square. Each entrance was covered by a grid of 0.005-in. stainless steel wire. After assembly on lavite (Lava A) supports, the cathode and three dynodes were oxidized in a two-step process.[10] A ten-stage commercial dynode structure (Dumont type 6292) was used in series with the special stages just described. Such structures were used in their standard glass envelopes after removal of the cathode end.[11] They were sealed to the main vacuum system by an *O* ring which slipped over the envelopes. The system was operated at 3000 to 4000 volts, half of which was between the fourth dynode (first commercial dynode) and the cathode. The latter was grounded to the vacuum tank. A sketch of the proton detector is shown in Fig. 2.

In our early experiments, the proton detector was placed relatively far away from the beam in order to reduce the general background. The protons were focussed onto this detector by an electrostatic lens between the detector and the beam. We belatedly realized, however, that a large fraction of the protons missed the detector owing to the component of their recoil velocity normal to the accelerating field. It was, of course, the ratio of the accelerating potential to the recoil energy which determined this loss and the accelerating voltage was limited by the rapid rise in background at accelerating voltages higher than 10 kev. In order to avoid the loss of protons from this source, the detector described above was built and mounted in the position shown, relatively near the beam. Fortunately, the background was not excessive in this position; in fact the ratio of number of observed neutron decays to background counts was higher than in the earlier arrangement.

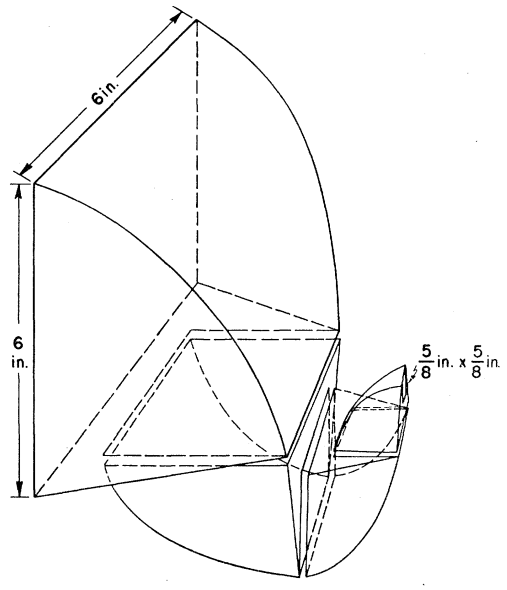

FIG. 2. Special silver-magnesium dynodes of the proton detector. These precede a commercial dynode structure which faces the $\frac{5}{8}$ in.$\times\frac{5}{8}$ in. exit.

[10] Paul Rappaport, J. Appl. Phys. **25**, 288 (1954).
[11] K. Koyama and R. E. Connally, Rev. Sci. Instr. **28**, 833 (1957).

D. Electron Detector

The detector for beta particles was a scintillator, 5 in. in diameter and 0.2 in. thick, consisting of a mosaic of 16 matched $1\frac{1}{4}$-in. square anthracene crystals cemented to each other and to a $\frac{1}{4}$-in. Lucite backing with a cold-setting epoxy resin and trimmed to approximately circular shape.

The Lucite backing was cemented to a Lucite light pipe, 6 in. long$\times$5 in. in diameter, which in turn was cemented to a 5-in. Dumont photomultiplier, type 6364. The light pipe allowed the photomultiplier to be mounted in a region where it could be adequately protected from the guide field with μ metal and iron shields.

The energy resolution of the anthracene mosaic was initially 17% for Cs^{137} electrons, but subsequent reduction in the uniformity of the photosurface worsened the resolution. Nevertheless, the signal-to-noise ratio in the energy window was better for this crystal than for the plastic scintillator tried.

The β-detector system could be mounted either on top of the vacuum chamber so as to look down at the narrow edge of the beam, or at the side of the tank so as to look at the width of the beam. In either position, the geometrical efficiency was about 3%.

E. Electronics

A schematic diagram of the electronic system is shown in Fig. 3. The heart of the system is a sequence-sensitive time-overlap circuit (time converter)[12] utilizing 2-μsec pulses from trigger pairs actuated by fast pulses from the detectors. The output of this circuit is linearly proportional to the overlap of the trigger pulses, and is sent to a 256-channel analyzer if the electron pulse preceeds the proton pulse by at least 0.02 μsec. In addition, selection of pulse sizes is made by single-channel pulse-height analyzers which analyze "slow" pulses from the detectors. The 256-channel analyzer is gated by coincidence of these single-channel analyzers. In the 256-channel analyzer, the output of the overlap circuit can be stored in one set of 128 channels if there is an "overcount" pulse from one of the analyzers and in the other set of 128 if there is not. The analyzer which controls this selection can be chosen for a particular experiment. This "overcount" pulse is

[12] Designed by R. Epstein of this laboratory.

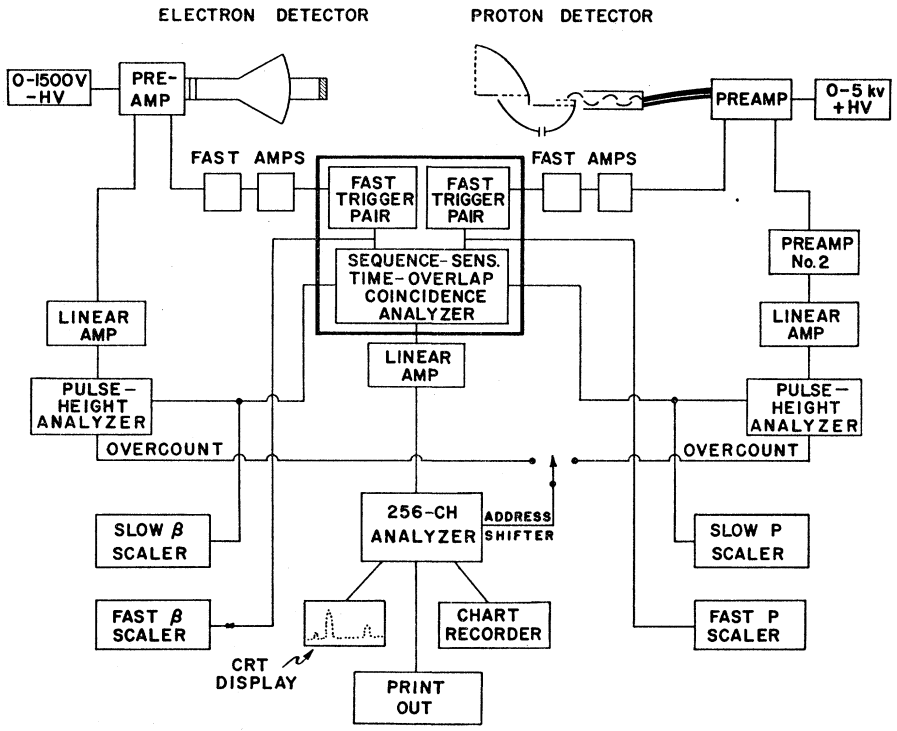

FIG. 3. Schematic diagram of electronic circuits.

emitted from either single-channel analyzer when a pulse exceeds the upper edge of its window. This allows breaking up either detector spectrum into two parts.

The results of a typical good 24-hr run are shown in Fig. 4. Prompt coincidences from background photons give maximum pulse-height corresponding to maximum pulse overlap. Increasing delay of the pulse from the proton detector is measured to the right from the prompt peak. The neutron peak appears at a delay of about 0.1 μsec, which is the expected drift time of the protons to the detector. The flat distribution is the accidental background.

III. CORRELATION OF ANTINEUTRINO MOMENTUM AND NEUTRON SPIN

This correlation is measured by observing the direction of the recoil protons relative to the direction of neutron spin for an electron momentum normal to the spin. The experimental arrangement used is illustrated in Fig. 5, a vertical cross section of the system. For this measurement the neutrons were polarized in the vertical direction. Consider for definiteness the case in which the neutron spins are pointing upward. In this case, if the antineutrino is emitted along the spin direction, the recoil proton receives a downward component of momentum and may be passed by the slits. When the neutron spins are reversed, the protons associated with antineutrinos emitted parallel to the spin are discriminated against by the slits. Thus, from the change in concidence rate with the two opposite neutron polarizations, the sign and magnitude of the correlation coefficient $\mathfrak{B}$ between the antineutrino momentum and the neutron spin can be obtained.

In practice, two measurements with reversed neutron polarization are not compared directly with each other since they involve a reversal of the magnetic fields which could conceivably affect the efficiencies of the

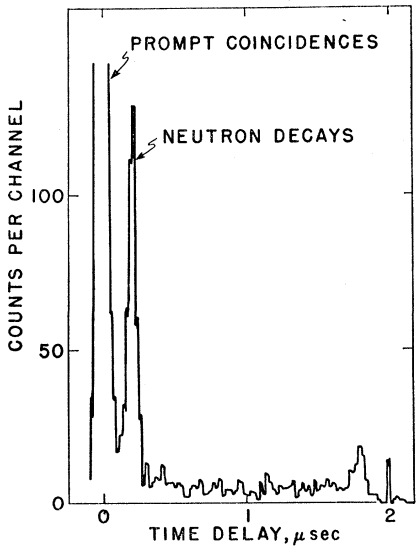

FIG. 4. Record of stored pulse-height spectrum from a typical run of about 8 hr in the experiment to measure $\mathfrak{A}$, the coefficient of the correlation between the spin direction and the direction of electron emission. About 100 channels are shown.

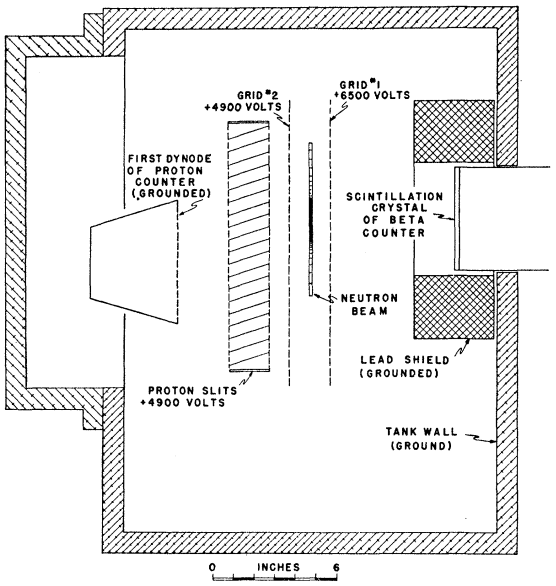

FIG. 5. Detector arrangement for measurement of the correlation $\mathfrak{B}$ between the directions of neutron spin and antineutrino momentum.

detectors. Instead, one compares measurements with a polarized and an unpolarized beam. The depolarization (as mentioned earlier) is achieved by inserting a steel sheet about 0.01 in. thick in the beam at a point at which the magnetic field is less than 100 gauss. Such a sheet appears to have no appreciable effect on the magnetic fields near the detectors and hence makes an ideal depolarizer. Such polarized-depolarized sequences were performed with both field (spin) directions, and the total effect was taken as the algebraic sum of these two differences.

The results of this experiment are shown in Table I, in which $\mathfrak{B}$ is the usual correlation coefficient of the cosine of the angle between the directions of interest. The errors given in the first line are statistical, while those in the last lines include an allowance for the estimated uncertainty in the correction factors.

There is a possibility that the slits may have a finite reflectivity for protons; if so this would reduce the observed value of the asymmetry. The value of $\mathfrak{B}$ reported here thus constitutes a lower bound.

In practice, the idealized considerations given in the introductory paragraph of this section do not apply to the geometry used. We therefore had to compute a geometrical correction factor. The procedure for this calculation, performed numerically on a computer, was as follows.

For a given position of decay in the beam region, given electron energy, and given electron direction, we calculated the number of antineutrinos that would yield protons of the proper trajectory to pass the slits and hit the detector. This was done for an isotropic distribution of antineutrinos and for one varying with $\cos\theta_{J,p_\nu}$, the same number of cases being considered in each distribution. The computation was then repeated for a series of possible electron directions (the spacing of the directions being varied to reflect the small anisotropy in the directions of emission of electrons, relative to the spin direction) in order to perform an integration over the surface of the electron detector. The entire calculation was then repeated for a series of decay positions in the beam. By averaging over the cross section of the beam, one obtains the counting rates to be expected for a fixed electron energy. This calculation was performed for eight equally spaced electron energies from 150 to 650 kev. The results were then averaged over the two parts of the beta spectrum accepted by the detector (150–350 kev and 350–780 kev), account being taken of the resolution of the scintillator and the beta spectrum.

The geometrical correction factor was obtained from the values calculated for the number of protons detected from the isotropic and from the $\cos\theta_{J,p_\nu}$ distributions. It is, in fact, the ratio of the two numbers. The numerical integrations involved in these calculations are reliable to a few percent. The calculated values of $\mathfrak{B}_{\text{exp}}$ are shown in Table I as a function of electron energy. The final $\mathfrak{B}_{\text{exp}}$ is not much affected by the poor energy resolution in the 150–350-kev region as the correction does not vary rapidly in this region. In the higher energy region the resolution correction is more reliably made and hence the resolution of the scintillator does not introduce a serious error although the correction is more strongly energy dependent here. The quoted uncertainty in the anisotropy coefficient $\mathfrak{B}$ includes a generous allowance for possible uncertainties in the correction factors.

IV. CORRELATION OF BETA-PARTICLE MOMENTUM AND NEUTRON SPIN

The arrangements for this experiment differed from that described in the preceding section in two important respects. First, the proton slits were removed, and second, the guide field and thus the direction of neutron polarization was turned horizontal. With this orientation of the neutron polarization, the observed strong correlation between the neutron spin and the proton recoil had a comparatively small effect on the relative efficiency with which protons were collected in the two

TABLE I. Results of measurements on the correlation between the momentum of the antineutrino and the neutron spin; $\omega=1+\mathfrak{B}(\mathbf{P}_{\bar{\nu}}/E_{\bar{\nu}})\cdot(\langle\mathbf{J}\rangle/J)$.

Beta energy group	150–350 kev	350–780 kev
Observed $\mathfrak{B}$	0.36±0.04	0.33±0.04
Geometrical correction factor	2.00±0.06	2.40±0.07
Correction factor for imperfections of polarization	1.15±0.1	1.15±0.1
$\mathfrak{B}$	0.83±0.25	0.91±0.19
Average $\mathfrak{B}$	0.88±0.15	

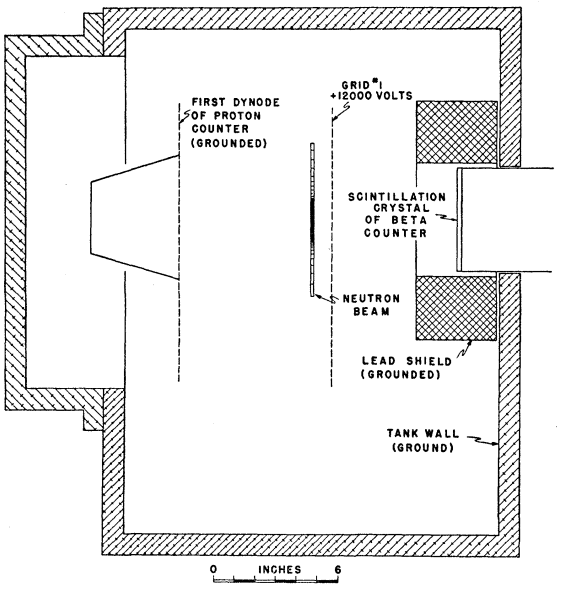

FIG. 6. Detector arrangement for the measurement of the correlation $\mathfrak{D}$ between the directions of neutron spin and electron momentum.

neutron spin directions used (toward and away from the beta counter). Figure 6 shows a cross section through the beam and vacuum tank with this arrangement in place.

It proved to be quite simple to rotate the plane of the polarized neutrons after they left the polarizing mirror. It was sufficient to provide a horizontal guide field by means of a magnetic condenser as mentioned before. The plates of this condenser ran the full length of the vacuum chamber. This left a rather short transition region in which the neutron spins were turned 90° since the vertical field of the polarizer was extended along the beam to within about 4 in. of the vacuum chamber by inserting steel plates $\frac{1}{2}$ in. thick by 6 in. wide (across the beam) above and below the beam. When the polarization of the beam was measured, the field of the analyzer was made vertical and the latter was placed about as far away from the guide-field plates as the polarizer so that the neutron spins rotated back to the vertical as they traversed the space from guide to analyzer. The results of the polarization measurement with this arrangement were the same as with the fields vertical between analyzer and polarizer.

A small correction to the results of this measurement is necessary because of an effect of the strong correlation $\mathfrak{B}$ between antineutrino momentum and neutron spin. This effect arises as follows. Because of the $\mathfrak{B}$ correlation, neutrons with their spins pointed toward the beta detector tend to give protons whose recoil direction is away from the beta counter. Thus, these protons will travel to the proton counter slightly faster on the average than those coming from neutrons oriented oppositely. (They travel only slightly faster because the proton recoil energy is, on the average, only a few percent of the accelerating potential applied by the grids.) Since both groups of protons receive the same component of recoil momentum perpendicular to the accelerating field, the faster moving ones are less apt to be deflected enough to miss the proton detector and hence will be collected more efficiently.

The actual corrections were made by the following numerical calculation performed on a computer. For each position from which the decay of a neutron in the beam could be detected, the trajectory of the recoil proton was calculated for each of several representative directions of emission of the electron and of the antineutrino. The fraction that missed the proton detector was computed by integrating over the sensitive volume, the range of angles over which the beta rays were detectable, and the known distribution of directions of emission of antineutrinos. As expected, the correction for the difference in collection efficiency for the two directions of polarization turned out to be smaller than the statistical uncertainty in the measurement.

In addition to this correction for the effects of $\mathfrak{B}$, a further correction is of course necessary for the direct effect of the finite size of the electron detector in reducing measured anisotropies. The results of this experiment, together with all pertinent corrections, are collected in Table II.

V. TEST OF INVARIANCE UNDER TIME REVERSAL

This test was performed by looking for a preference of the antineutrino emission for one side or other of the plane determined by the directions of electron momentum and neutron spin, i.e., the term proportional to $\langle \mathbf{J} \rangle \cdot (\mathbf{p}_e \times \mathbf{p}_{\bar{\nu}})$. The experimental arrangements were those used in measuring the correlation of the antineutrino momentum and the neutron spin (Fig. 5), with one change. The proton slits were rotated 90° about an axis running from the center of the beta counter to the center of the proton counter. The slits thus discriminated between protons moving with a component of momentum parallel or antiparallel to the direction of the neutron beam, a direction perpendicular to both $\langle \mathbf{J} \rangle$ and $\mathbf{p}_e$. The measurement as usual consisted

TABLE II. Results of the measurement on the correlation between the momentum of the beta particle and the neutron spin; $\omega = 1 + \mathfrak{a}(\mathbf{p}_e/E_e) \cdot (\langle \mathbf{J} \rangle / J)$.

Beta energy group	150–780 kev
Observed $\mathfrak{a}$	-0.066 ± 0.010
Correction factor for contribution from correlation of neutron spin and proton momentum (antineutrino asymmetry)	1.12 ± 0.03
Correction factor for imperfections of polarization	1.19 ± 0.1
Geometrical correction factor	1.07 ± 0.02
Correction factor for beta velocity, c/v	1.20 ± 0.06
$\mathfrak{a}$	-0.114 ± 0.019

TABLE III. Results of measurements on the correlation between antineutrino momentum $p_{\bar{\nu}}$, electron momentum p_e, and neutron spin, $\langle \mathbf{J} \rangle$;

$$\omega = 1 + \mathfrak{D} \frac{\langle \mathbf{J} \rangle}{J} \cdot \frac{\mathbf{p}_e}{E_e} \times \frac{\mathbf{p}_{\bar{\nu}}}{E_{\bar{\nu}}}.$$

Beta energy group	150–650 kev
Observed asymmetry	-0.015 ± 0.019
Geometrical correction factor	1.7 ± 0.3
Correction factor for imperfection of polarization	1.15 ± 0.1
Correction factor for beta velocity, $c/\bar{v}$	1.25 ± 0.07
$\mathfrak{D}$	0.04 ± 0.05

of a comparison of the delayed coincidence counting rates with polarized and unpolarized neutron beams. These measurements were also made with the fields, and hence polarization of the neutrons, reversed. The observed asymmetry given in Table III is the average of all these measurements, with due account taken of signs.

The correction of these results for the effects of finite dimensions of the apparatus and imperfections of polarization was very similar to that for the measurements of $\mathfrak{B}$. The calculation of the correction factor proceeds exactly as in the antineutrino case except that the effect of the $\mathfrak{B}$ correlation must be included. These calculations indicate that, because of the effect of $\mathfrak{B}$ on the $\mathfrak{D}$ correction factor, the latter is about 20% less than in the $\mathfrak{B}$ experiment.

The electron and antineutrino asymmetries will contribute to the apparent three-vector term if the average angle between the neutron spin and the direction of emission of the detected electrons is not 90°, or if the plane of the proton slits is not parallel to the direction of neutron spin. The latter effect is more serious as the neutrino asymmetry coefficient is ten times as large as that for the electron. The effect will enter roughly as the sine of the angle of deviation from the parallel situation, so that a deviation of 1° will change $\mathfrak{D}$ by ± 0.008. The apparatus was carefully lined up so this uncertainty in angle is about 1° or less.

There was also a correction for the average $p_e/E = v/c$ of the beta spectrum. Applying all these corrections to the experimental result, we obtain the result given in the last line of Table III. This value of $\mathfrak{D}$ indicates that there is no significant failure of invariance under time reversal.

VI. DISCUSSION

Since the neutron is one of the simplest entities showing β decay, it would be quite interesting to try to determine all the fundamental parameters of β decay by the use of data from the neutron decay only. Unfortunately, the present accuracy and completeness of the data do not make this practicable. It is therefore necessary to use data from other forms of β decay and assumptions about the character of the decay. The customary approach starts from the angular distribution expression, Eq. (2), given by Jackson, Treiman, and Wyld,[3] in the derivation of which it was assumed that special relativity applies to the description of electrons and antineutrinos and that only a point interaction is involved. Now the results of measurements on the longitudinal polarization of electrons and positrons (which give agreement with a polarization equal to v/c) and the absence of Fierz terms (as shown best by ratios of K capture to positron emission) show that $S = -S'$, $V = V'$, $T = -T'$ and $A = A'$. The expressions for the asymmetry coefficients then become

TABLE IV. Predicted values for $\mathfrak{A}$ and $\mathfrak{B}$.

Combination of coupling coefficients	$S+T$	$S-T$	$V+A$	$V-A$	Exp.
$\mathfrak{A}$	-1	-0.10	-1	-0.10	-0.11
$\mathfrak{B}$	-0.10	-1	0.10	$+1$	$+0.88$

$$\mathfrak{A} = \frac{-2\,\mathrm{Re}(|T|^2 + |A|^2 + ST^* + VA^*)}{|V|^2 + |S|^2 + 3|T|^2 + 3|A|^2},$$

$$\mathfrak{B} = \frac{-2\,\mathrm{Re}(|T|^2 - |A|^2 - ST^* + VA^*)}{|V|^2 + |S|^2 + 3|T|^2 + 3|A|^2}, \qquad (4)$$

$$\mathfrak{D} = \frac{2\,\mathrm{Im}(ST^* - VA^*)}{|V|^2 + |S|^2 + 3|T|^2 + 3|A|^2}.$$

(We use T where Jackson, Treiman, and Wyld use C_T, A for C_A, etc.) Complex coupling coefficients allow for the possibility of failure of invariance under time reversal. On the basis of our measurement of $\mathfrak{D}$, however, it seems reasonable to take all coefficients as real. Such values of $\mathfrak{A}$ and $\mathfrak{B}$, calculated for four possible combinations of coupling coefficients, are given in Table IV. In calculating this table, the ratio of Gamow-Teller to Fermi matrix elements, $|GT|^2/|F|^2$, was taken to be 1.42, the result inferred from the measured lifetime of the neutron[13] and from the ft value of O[14].

Obviously other linear combinations of these coefficients are conceivable and the table serves chiefly to illustrate the sensitivity of these calculations of $\mathfrak{A}$ and $\mathfrak{B}$ to changes in the assumed mixture.[14] However, if we assume that any of the coupling coefficients is either completely absent or else present in nearly the same strength (absolute value) as any other, then the $A-V$

[13] A. Sosnovskii, P. Spivak, Yu. Prokofiev, T. Kutikov, and Yu. Dobrinin, Nuclear Phys. **10**, 395 (1959).

[14] It should be noted that under the conditions $S = -S'$, $V = V'$, $A = A'$, $T = -T'$, the occurrence of only V and A implies the emission of a right-handed antineutrino and of only S and T the emission of a left-handed antineutrino; whereas a mixture of these pairs, such as $V+T$ or $S+V+T+A$ would imply a mixed handedness. See, for example, M. Gell-Mann and A. H. Rosenfeld, *Annual Reviews of Nuclear Science* (Annual Reviews, Inc., Palo Alto, California, 1957), Vol. 7, p. 407.

combination is the only one that agrees with these experiments.

The value $|GT|^2/|F|^2=1.55\pm0.1$ obtained from our value of $\mathfrak{A}$ is in reasonable agreement with that obtained from the neutron lifetime but is not in agreement with the value (1.16 ± 0.05) obtained[15] from ft values of the mirror nuclei O^{15}, F^{17}, and Ca^{39}.

It may be of more than academic interest to relax the assumption that there are no small terms in the interaction and attempt to use the data from this experiment to put rough limits on these small contributions. If the substitutions

$$a=|S|/|V|,\quad S^2=a^2V^2;\quad b=|T|/|A|,\quad T^2=b^2A^2;$$
$$\mathrm{Re}(ST^*)=|S||T|\cos\phi_{ST}=ab|V||A|\cos\phi_{ST};$$
$$\mathrm{Re}(VA^*)=|V||A|\cos\phi_{VA},$$

are made in Eqs. (4), the values of $|A|/|V|$ obtained from the first two are

$$\frac{|A|}{|V|}=\frac{\mathfrak{A}(1+a^2)}{-(ab\cos\phi_{ST}+\cos\phi_{VA})\pm[(ab\cos\phi_{ST}+\cos\phi_{VA})^2-\mathfrak{A}(1+a^2)(1+b^2)(2+3\mathfrak{A})]^{\frac{1}{2}}}$$

and

$$\frac{|A|}{|V|}=\frac{\mathfrak{B}(1+a^2)}{(ab\cos\phi_{ST}-\cos\phi_{VA})\pm\{(ab\cos\phi_{ST}-\cos\phi_{VA})^2-\mathfrak{B}(1+a^2)[3\mathfrak{B}(1+b^2)-2(1-b^2)]\}^{\frac{1}{2}}},$$

respectively. The equation for $\mathfrak{D}$ yields

$$ab\sin\phi_{ST}-\sin\phi_{VA}=\left[\frac{|V|}{|A|}(1+a^2)+3\frac{|A|}{|V|}(1+b^2)\right]\frac{\mathfrak{D}}{2}.$$

Now we may see what ranges of a, b, ϕ_{ST}, and ϕ_{VA} will give reasonable values of $|A|/|V|$ and of

$$\frac{|GT|}{|F|}=\frac{(T^2+A^2)^{\frac{1}{2}}}{(S^2+V^2)^{\frac{1}{2}}}=\left(\frac{1+b^2}{1+a^2}\right)^{\frac{1}{2}}\frac{|A|}{|V|},$$

under the boundary conditions that a and b are smaller than unity and ϕ_{ST} and ϕ_{VA} are not far from 180,° i.e., the interaction is predominantly $A-V$. This assumption means that $\cos\phi\approx-1$ so that the calculations involving $\mathfrak{A}$ and $\mathfrak{B}$ are not very sensitive to variations in ϕ.

In Figs. 7–9 are shown the ranges of values of $|GT|/|F|$ obtained for the experimental ranges of $\mathfrak{A}$ and $\mathfrak{B}$ for the three sets of assumptions given in the figures. In Fig. 10 are shown the ranges of values of ϕ obtained for the experimental range of $\mathfrak{D}$ under the four sets of assumptions shown. In calculating Fig. 10, $|GT|/|F|$ was assumed to be 1.25 but the calculation is not at all sensitive to this assumption. From this figure we conclude that the possible phase deviation from 180° is little affected by the various types of contributions of S and V considered. Conversely, the cosines of possible phase angles are nearly ±1 so that a small breakdown of time reversal in this region would not greatly affect the earlier analysis which involved $\mathfrak{A}$ and $\mathfrak{B}$. Thus the assumption of $\phi=\pi$ seems adequate. Other sets of assumptions are of course possible but a more exhaustive analysis of the possibilities should probably await more precise data on $\mathfrak{A}$, $\mathfrak{B}$, and $\mathfrak{D}$.

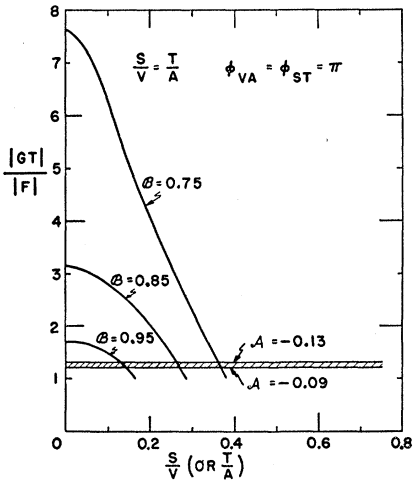

FIG. 7. The range of $|GT|/|F|$ obtained for the experimental range in the coefficients $\mathfrak{A}$ and $\mathfrak{B}$ under the assumptions shown.

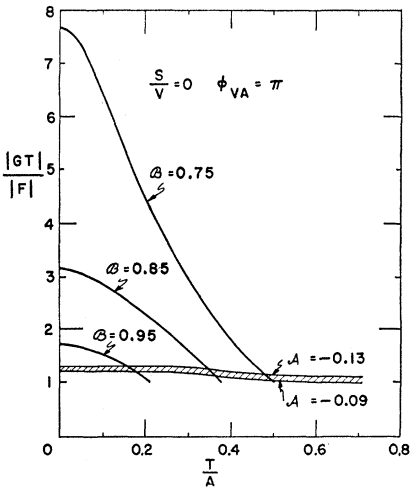

FIG. 8. The range of $|GT|/|F|$ obtained for the experimental range in the coefficients $\mathfrak{A}$ and $\mathfrak{B}$ under the assumptions shown.

[15] O. C. Kistner and B. M. Rustad, Phys. Rev. **114**, 1329 (1959).

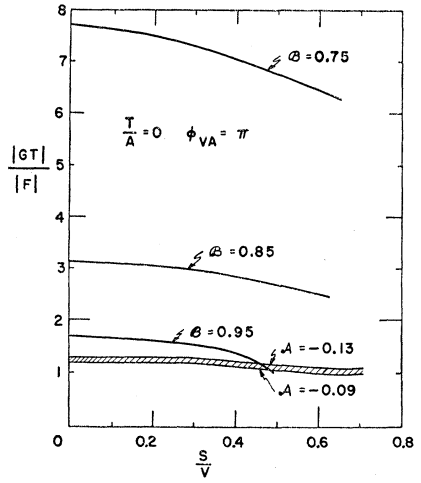

FIG. 9. The range of $|GT|/|F|$ obtained for the experimental range in the coefficients $\mathfrak{A}$ and $\mathfrak{B}$ under the assumptions shown.

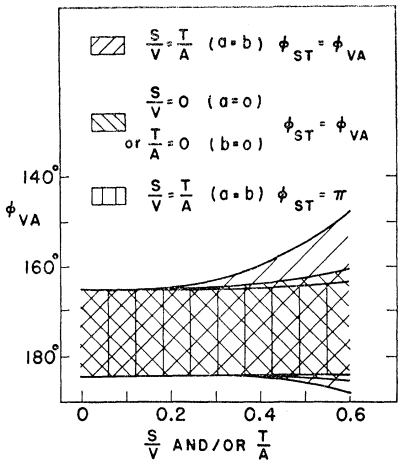

FIG. 10. The range in ϕ_{VA} obtained for the experimental range of coefficient $\mathfrak{D}$.

In conclusion, the following statements can reasonably be made about the nature of the beta decay of the neutron:

a. The parity operation is not an invariant operation in neutron decay.

b. The time reversal operation is an invariant operation in neutron decay or, more precisely, the relative phase angle between the interaction amplitudes of the vector and axial vector types is $175°\pm10°$.

c. The vector and axial vector types of interaction predominate with a probable maximum contribution of about 30% of scalar and tensor type of coupling.

d. The vector and axial vector types of interaction contribute in the ratio $A^2/V^2=1.55\pm0.1$ or $|A|/|V|=1.25\pm0.05$.

e. The antineutrino is right handed; the direction of spin lies along the direction of momentum.

These conclusions are also consistent with the results reported by Clark and Robson[16] although their accuracies do not appear to be as good as those we have claimed for our experiments.

ACKNOWLEDGMENTS

We are very much indebted to many of our colleagues at Argonne National Laboratory for aid much beyond the routine in performing these experiments. Without minimizing the values of the help received from any of the others, we feel we must mention especially Mr. M. T. Burns of the Central Shops, Mr. R. J. Epstein of Electronics, and Dr. S. Raboy of the Physics Division.

We are also very grateful for the advice and aid received from Dr. B. Stech of the University of Heidelberg.

[16] M. A. Clark and J. Robson, Can. J. Phys. **38**, 693 (1960).